AIAA 82-4078

An Adaptive Stick-Gain to Reduce Pilot-Induced Oscillation Tendencies

Bruce G. Powers*
NASA Dryden Flight Research Center, Edwards, Calif.

As part of a program to improve the approach and landing characteristics of the space shuttle, an adaptive algorithm that varies the longitudinal stick gearing has been developed to reduce the shuttle's tendency for pilot-induced oscillation (PIO). This paper describes the algorithm, which is known as the PIO suppressor, and discusses some of the tradeoffs involved in optimizing the system. The results of fixed-base, moving-base, and in-flight simulations of the PIO suppressor are presented.

Nomenclature

A	= amplitude
a,b,c,d	= suppressor constants (Fig. 1)
a_2	= suppressor constant (Fig. 9)
CW	= XK gain schedule variable
h	= main gear wheel height, ft
k	= index parameter
q	= pitch rate, deg/s
$q_{t=0.8}$	= responsiveness, pitch rate at $t=0.8$ s for step input by pilot, deg/s
s	= Laplace transform operator
T	= digital system sample interval, s
t	= time, s
t_k	= arbitrary time, point of interest, s
W	= PIO suppressor variable
$W_{\min}$	= XK gain schedule variable
XK	= suppression factor
$\overline{XK}$	= suppression, steady-state value of XK for input of 2.5 rad/s
$XK_{\min}$	= XK gain schedule variable
δ	= output of stick deadband, deg
δ_c	= output of stick shaping, deg
δ_e	= elevator deflection, deg
δ_p	= pitch controller deflection, deg
ω	= frequency, rad/s

Introduction

DURING the approach and landing flight testing of the space shuttle, a tendency for pilot-induced oscillation (PIO) was observed during the landing phase of the flights.[1] Subsequent analysis indicated a potential PIO tendency in the pitch axis. Factors contributing to the PIO tendency included excessive lags in the digital flight control system, poor visual and motion cues due to the cockpit location, and the high-gain task of landing an unpowered vehicle on a runway.

As part of a program to improve the shuttle's landing characteristics, a nonlinear adaptive filter was developed to reduce the shuttle's PIO tendencies. This filter, known as a PIO suppressor, adaptively changes the longitudinal stick gearing whenever the pilot approaches a PIO situation. This paper describes the basic PIO suppressor developed in Ref. 2, two modified versions of that suppressor, and an alternate formulation of the suppressor algorithm. The results of several simulations conducted during the development and evaluation of the PIO suppressor concept are also presented.

Received Feb. 4, 1981; revision received July 17, 1981. This paper is declared a work of the U.S. Government and therefore is in the public domain.

*Aerospace Engineer. Member AIAA.

Baseline PIO Suppressor

To suppress the PIO tendencies, it was necessary to attenuate pilot inputs near the PIO frequency (approximately 2.5-3.0 rad/s). Because attenuation is accompanied by additional phase lag, and because one of the major causes of the shuttle's PIO was the phase lag in the control system, an ordinary linear filter could not be used. The objective in the development of the PIO suppressor was to provide the required attenuation without increasing the phase lag.

Most of the development of the baseline PIO suppressor[2] was done on a fixed-base simulator using an air-to-air tracking task rather than the landing task. The tracking task could be used to artificially create a high-gain situation that made the PIO tendencies of various configurations more obvious to the evaluation pilot. By varying the simulated distance between the tracking vehicle and the target, the relative gain between the altitude tracking and the attitude tracking could be controlled. Thus, by adjusting the tracking distance, it was possible to define a task that reproduced the pilot-in-the-loop frequencies observed during the landing phase of flight tests of the space shuttle.

A block diagram of the suppressor is shown in Fig. 1. The general operation involves the estimation of the dominant frequency of the pilot input and the scheduling of the pilot stick shaping as a function of the estimated frequency. To understand the detailed operation of the PIO suppressor, consider a sinusoidal pilot input, $A\sin\omega t$. The magnitude of this signal is A. The derivative is $\omega A\cos\omega t$, which has a magnitude of ωA. In the amplitude path of the PIO suppressor (Fig. 1), the magnitude of the pilot input is determined by smoothing the squared signal to obtain the root mean square (rms) value of A. In the amplitude-frequency path, the lead-lag filter and differencing network provides a dif-

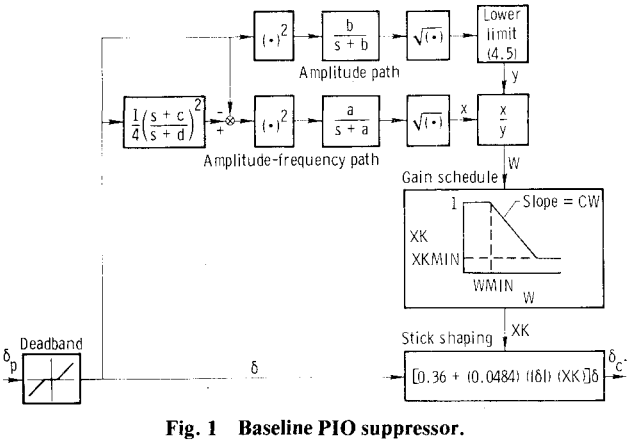

Fig. 1 Baseline PIO suppressor.

Table 1 Values of baseline and modified baseline PIO suppressor constants[a]

Constant	PIO suppressor Baseline	Modified baseline D-1	Modified baseline D-3
a	0.30	0.65	0.65
b	0.3	1.0	1.0
c	20.0	6.0	6.0
d	10.0	3.0	3.0
CW	−3.850	−2.174	−1.667
W_{min}	0	0.16	0.20
XK_{min}	−0.15	0	0

[a] Constants are defined in Fig. 1

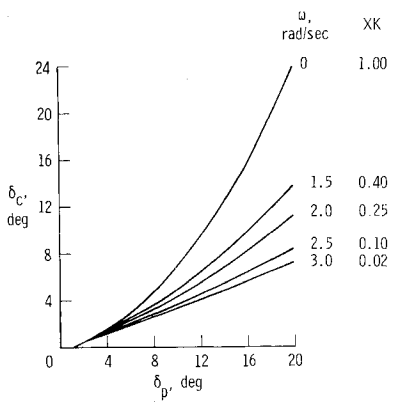

Fig. 2 Example of frequency-dependent stick shaping.

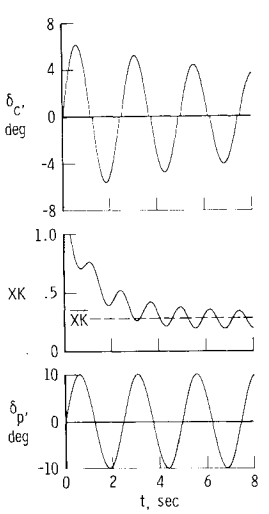

Fig. 3 Example of response to sinusoidal input with PIO suppressor.

ferentiation of the input signal below a frequency of d. This result is then squared and smoothed to obtain the rms value of ωA. The constants a and b are chosen to provide approximately constant signals proportional to amplitude and amplitude-frequency values. The ratio of the two signals is then proportional to the frequency. A gain schedule is used to modify the parabolic term in the stick shaping equation. Figure 2 shows a typical example of the resulting stick shaping. The constants for the baseline PIO suppressor are given in Table 1. The PIO suppressor is implemented digitally in the shuttle flight control system with a rate of 25 samples/s.

Responsiveness/Suppression Tradeoffs

The PIO suppressor is time varying and nonlinear. A typical response to a sinusoidal input is shown in Fig. 3. In this case, the input is a 50% (10 deg) pitch control deflection

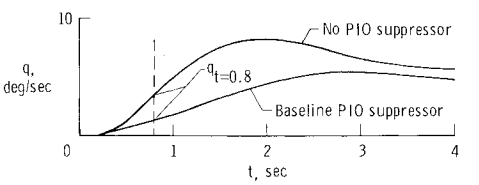

Fig. 4 Example of reduction in step response with baseline PIO suppressor, δ_p = 15-deg step (20-deg maximum).

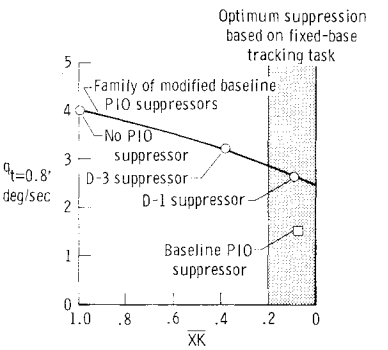

Fig. 5 Responsiveness/suppression tradeoffs.

at a frequency of 2.5 rad/s. The suppression factor XK and stick shaping output δ_c approach steady-state values after about one to two cycles of the input. The average steady-state value of XK can be used as an indication of the amount of suppression and is referred to as $\overline{XK}$.

From a response standpoint, it would be desirable for normal inputs (that is, those not at the PIO frequency) to have the same effect as if the PIO suppressor were not present. However, the baseline PIO suppressor had an adverse effect on step response, as shown in Fig. 4. In this case, a large step was input where no previous inputs had been made ($XK = 1.0$ at $t = 0$). For comparison purposes, the pitch rate at $t = 0.8$ s is used as a measure of the response characteristics and is referred to as the responsiveness. For the baseline PIO suppressor, the responsiveness is about half that without the PIO suppressor. Preliminary pilot evaluations indicated that this loss in responsiveness would be unacceptable.

The effects of the suppressor parameters were studied in an effort to improve the response characteristics. The second-order filter (constants c and d in Fig. 1) provides the differentiation of the input signal. By changing the constants from $c = 20$ and $d = 10$ to $c = 6$ and $d = 3$, the frequency range of the differentiator was reduced from about 10 to 3 rad/s. This change reduced the effect of the higher frequency inputs found in a step input. Further improvements in the step response were made by reducing the time constants in the smoothing filters and by lagging the amplitude-frequency path relative to the amplitude path. These changes resulted in a family of modified baseline suppressors.

The responsiveness/suppression tradeoffs possible with the family of modified baseline PIO suppressors are shown in Fig. 5. These tradeoffs are obtained by varying the XK-vs-W gain schedule of Fig. 1. Also shown in Fig. 5 are the results obtained with the baseline PIO suppressor and two particular modified baseline suppressors, D-1 and D-3, which were investigated in depth. The optimum amount of suppression, based on pilot comments from the fixed-base simulation, corresponded to a value of $\overline{XK}$ ranging from 0 to 0.2.

In-Flight Simulation

Although the tracking task provided a good assessment of the PIO tendency, it did not provide a good indication of the significance of the responsiveness. As a result, two modified PIO suppressor configurations were evaluated in flight using the Calspan Total In-Flight Simulator (TIFS) variable

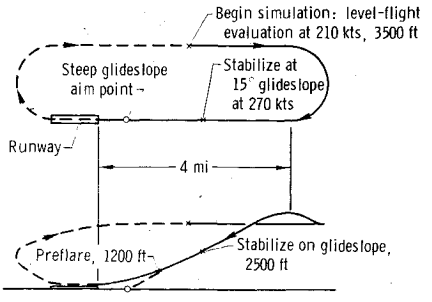

Fig. 6 Test pattern for TIFS simulation.

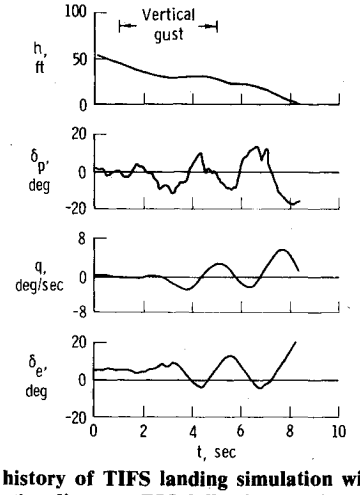

Fig. 7 Time history of TIFS landing simulation without PIO suppressor, illustrating divergent PIO following gust input.

stability airplane. The first configuration, D-1, provided the optimum suppression based on the fixed-base simulation. The second configuration, D-3, was chosen as a compromise between responsiveness and suppression requirements. The constants used for these suppressors are shown in Table 1.

The Calspan TIFS variable stability airplane was used to simulate the space shuttle approach and landing from an altitude of about 2500 ft to a simulated touchdown, with the pilot's eye height above the runway in the simulator equal to that in the shuttle. The PIO suppressors were evaluated by seven pilots during 125 approaches. The test pattern is shown in Fig. 6. Preliminary assessments of each configuration were made on the downwind leg. To produce a more stressful landing task, thus increasing the likelihood of PIO, a 150-ft lateral offset correction was made at an altitude of about 200 ft, and a 15-ft/s discrete vertical gust was simulated at an altitude of about 50 ft. This represented an unrealistic task in terms of what would actually occur in flight, but it was a convenient method of introducing a high-gain task into the simulation. Further details of the simulation are reported in Ref. 3.

A time history of a landing without a PIO suppressor is shown in Fig. 7. In this case, a divergent PIO occurred while the pilot was attempting to correct for the vertical gust. The large pilot inputs generally led to elevator rate limiting, which further aggravated the PIO. A landing using the D-3 PIO suppressor is shown in Fig. 8. The oscillatory motion is significantly reduced. As the pilot begins to correct for the gust, the suppression increases, thus lowering the stick gain and allowing a satisfactory landing.

In general, the pilots found the basic shuttle without a PIO suppressor to have a definite PIO tendency under high-stress conditions. With the D-3 PIO suppressor, the PIO tendency was considerably reduced, although an overly aggressive control technique could still lead to a divergent PIO in some cases. With the D-1 PIO suppressor, there was almost no PIO

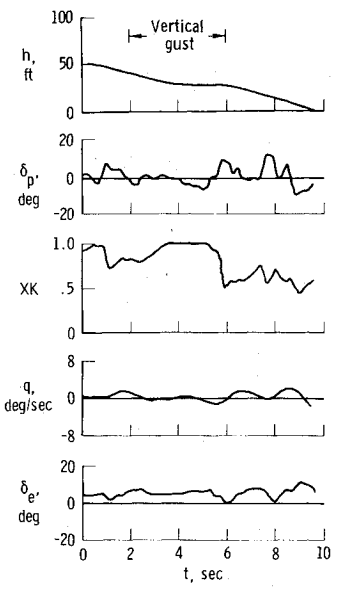

Fig. 8 Time history of TIFS landing simulation using D-3 modified PIO suppressor.

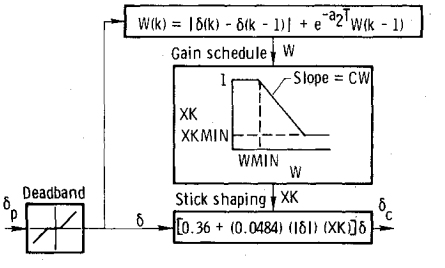

Fig. 9 Stick-rate PIO suppressor.

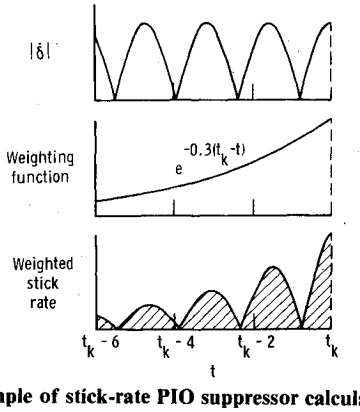

Fig. 10 Example of stick-rate PIO suppressor calculation: input δ is 10 sin (2.5t); area under curve (shaded) is $W(t_k)$.

tendency. However, the loss of responsiveness was noticeable, especially to the pilots with the most training on the basic configuration. As a result, the D-3 PIO suppressor was determined to be the best compromise between PIO protection and retraining requirements, and was selected for use on the first space shuttle entry flight.

Stick-Rate PIO Suppressor

To further improve the suppression/responsiveness tradeoff, and to improve the computational efficiency of the PIO suppressor, another algorithm was developed. Instead of estimating the pitch controller frequency, this algorithm measures average pitch controller rate and is referred to as the stick-rate PIO suppressor.

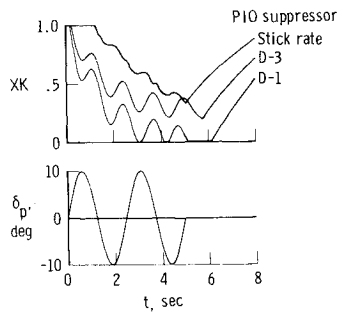

Fig. 11 Suppression characteristics for stick-rate and modified baseline PIO suppressors.

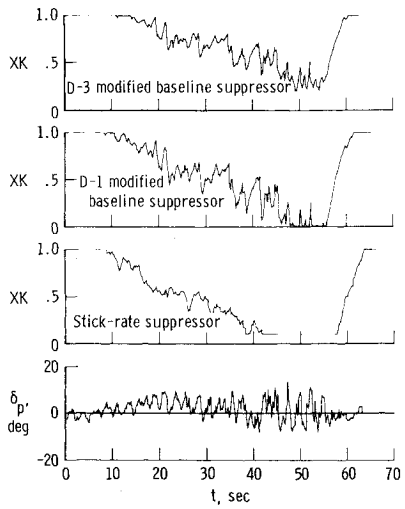

Fig. 12 Comparison of stick-rate and modified baseline PIO suppressors for typical pilot inputs.

A diagram of the suppressor is shown in Fig. 9. The parameter W is the average stick rate with an exponential deweighting of past values. This calculation is illustrated in Fig. 10. At any time, t_k, the value $W(t_k)$ is the area under the curve of the product of the absolute value of $\dot{\delta}$ and the exponential weighting function $e^{-a(t_k-t)}$. The absolute value performs a rectification function similar to the squaring function in the baseline suppressor. The exponential weighting performs a smoothing function similar to that of the first-order filters in the baseline suppressor. The value of W is used to compute XK using a gain schedule in the same manner as for the D-series PIO suppressors. The values of the constants used were $a_2 = 0.3$, $CW = -0.025$, $W_{\min} = 15.0$, and $XK_{\min} = 0.1$.

As shown in Fig. 11, the response with this suppressor to a sinusoidal input is similar to the baseline suppressor responses. Although the amount of suppression resulting from the sinusoidal input is considerably less than that with the baseline suppressor, the suppression resulting from actual pilot inputs was about the same as for the D-1 suppressor (Fig. 12). In Fig. 13, the pitch-rate responses to a step input for the stick-rate PIO suppressor are compared with those for the modified baseline suppressor. The response with the stick-rate PIO suppressor is essentially the same as the response without a suppressor. As a result, the desired amount of suppression can be chosen without compromising the step response for normal (low-stress) flying.

Moving-Base Simulation

To obtain additional experience with the D-3 modified baseline PIO suppressor, and to evaluate the stick-rate PIO suppressor, a moving-base simulation of the shuttle landing characteristics was conducted on the Ames Vertical Motion

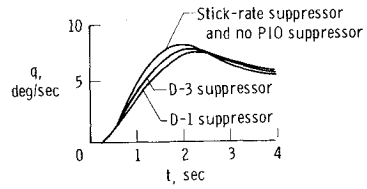

Fig. 13 Step response characteristics for stick-rate and modified PIO suppressors.

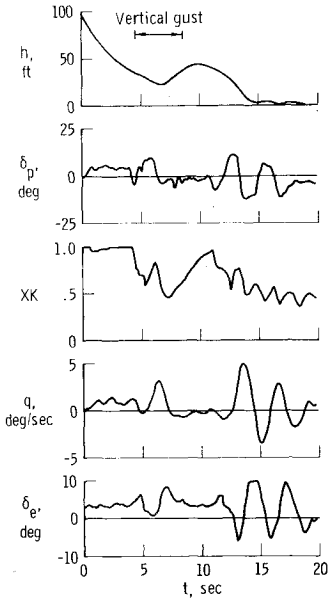

Fig. 14 Time history of VMS landing simulation using D-3 modified baseline suppressor.

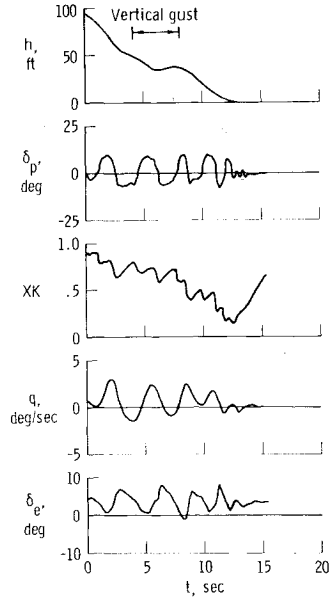

Fig. 15 Time history of VMS landing simulation using stick-rate PIO suppressor.

Simulator (VMS). Of particular importance was the capability for simulating the landing gear reactions so that touchdown bounce and nose-gear touchdown characteristics could be examined. The in-flight simulation tests had indicated that the greatest amount of suppression occurred at touchdown, but it was not known if any adverse effects would result during a bounce or during nose-gear letdown. The standard evaluation task was similar to that used in the TIFS simulation, with a lateral offset correction and a discrete vertical gust used to create a high-stress landing situation. In addition, various combinations of cross-winds and turbulence levels were evaluated.

A landing time history from the VMS simulation is shown in Fig. 14 for the D-3 modified baseline PIO suppressor. In this case, aggressive control led to a large oscillation in pitch rate shortly before touchdown. At that time, the suppression factor *XK* was reduced to a value between 0.4 and 0.5, and the pilot was able to reduce the oscillations and make a satisfactory touchdown. Over 300 landings were made during the VMS simulation for the D-3 modified baseline PIO suppressor. The results were similar to those of the TIFS program. The PIO tendencies were significantly reduced. No adverse effects of the PIO suppressor were encountered with the addition of the touchdown dynamics.

A time history of a landing with the stick-rate PIO suppressor is shown in Fig. 15. As the pilot activity increased near touchdown, the suppression increased in much the same manner as for the baseline suppressor. The oscillatory motion was reduced considerably and a satisfactory landing was made. Pilot comments indicated that with the stick-rate PIO suppressor, PIO tendencies were reduced considerably and were comparable to the tendencies with the D-1 PIO suppressor. The results indicated that the stick-rate PIO suppressor can provide the same desirable PIO suppression characteristics as the modified baseline suppressor, with a minimal effect on normal flying and increased computational efficiency.

Concluding Remarks

An adaptive stick-gain concept has been developed to reduce the space shuttle's tendency for longitudinal pilot-induced oscillations during the landing task. The adaptive stick-gain algorithms detect the type of pilot inputs that lead to oscillatory motions and reduce the longitudinal stick gain to a level where the pilot can maintain positive control and perform a satisfactory landing. The concept has been evaluated on fixed-base, moving-base, and in-flight simulations. The ability to significantly reduce PIO tendencies during high-stress landing tasks has been demonstrated, and an adaptive stick-gain algorithm has been implemented for use on the first space shuttle entry flight.

References

[1]Hoey, R.G. et al., "AFFTC Evaluation of the Space Shuttle Orbiter and Carrier Aircraft—NASA Approach and Landing Test," Air Force Flight Test Center, Edwards Air Force Base, Calif., AFFTC-TR-78-14, May 1978.

[2]Smith, J.W. and Edwards, J.W., "Design of a Nonlinear Adaptive Filter for Suppression of Shuttle Pilot-Induced Oscillation Tendencies," NASA TM-81349, April 1980.

[3]Weingarten, N.C., "In-Flight Simulation of the Space Shuttle (STS-1) During Landing Approach With Pilot-Induced Oscillation Suppressor," Calspan Rept. 6339-F-2, Dec. 1979.